Inorganic Chemistry

Article

pubs.acs.org/IC

Using Substituted Cyclometalated Quinoxaline Ligands To Finely Tune the Luminescence Properties of Iridium(III) Complexes

Emily E. Langdon-Jones, Andrew J. Hallett, Jack D. Routledge, David A. Crole, Benjamin D. Ward, James A. Platts, and Simon J. A. Pope*

School of Chemistry, Main Building, Cardiff University, Park Place, Cardiff CF10 3AT, United Kingdom

Supporting Information

ABSTRACT: The syntheses of five new heteroleptic iridium complexes $[\mathbf{Ir}(\mathbf{L}^{1-4})_2(\mathbf{Diobpy})]\mathbf{PF}_6$ (where Diobpy = 4,4′-dioctylamido-2,2′-bipyridine) and $[\mathbf{Ir}(\mathbf{L}^{3})_2(\mathbf{bpy})]\mathbf{PF}_6$ (where L = *para*-substituted 2,3-diphenylquinoxaline cyclometalating ligands; bpy = 2,2′-bipyridine) are described. The structures of $[\mathbf{Ir}(\mathbf{L}^{3})_2(\mathbf{Diobpy})]\mathbf{PF}_6$ and $[\mathbf{Ir}(\mathbf{L}^{3})_2(\mathbf{bpy})]\mathbf{PF}_6$ show that the complexes each adopt a distorted octahedral geometry with the expected *trans*-N, *cis*-C arrangement of the cyclometalated ligands. Electrochemical studies confirmed subtle perturbation of the $Ir^{III/IV}$ redox couple as a function of ligand variation. Luminescence studies showed the significant contribution of ^{3}MLCT to the phosphorescent character with predictable and modestly tunable emission wavelengths between 618 and 636 nm. DFT studies provided approximate qualitative descriptions of the HOMO {located over the Ir(5d) center (11−42%) and the phenylquinoxaline ligand (54−87%)} and LUMO {located over the ancillary bipyridine ligands (ca. 93%)} energy levels of the five complexes, confirming significant MLCT character. TD-DFT calculations indicate that UV−vis absorption and subsequent emission has substantial MLCT character, mixed with LLCT. Predicted absorption and emission wavelengths are in good general agreement with the UV−vis and luminescence experiments.

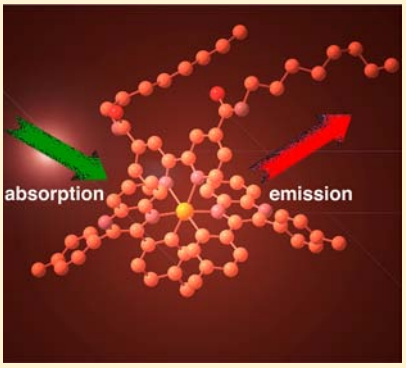

INTRODUCTION

Iridium(III) cyclometalated complexes have attracted increasing attention over the past 10 years due to their use in a range of photonic applications, such as phosphorescent organic light emitting diodes (OLEDs).[1,2] Typically, strong heavy metal mediated spin−orbit coupling results in efficient intersystem crossing from singlet to triplet excited states, resulting in high phosphorescent efficiencies. In reality, the effective commercialization of OLEDs requires emitters that address the breadth of the visible light spectrum from blue through green to red light.[3] Whereas green emitters, such as $[Ir(ppy)_3]$, have been well developed,[4] the lower band gap inherent to red emitters often results in lower luminescence quantum yields.[5] While the majority of reports of cationic Ir(III) complexes have been concerned with electroluminescent devices,[4,5] due to mobile counterions facilitating charge transport across films, there are several reports of their uses as dopants in OLEDs.[6]

Most of the early examples of iridium(III) cyclometalated complexes were based on the phenylpyridine orthometalating ligand,[7] although there have been more recent reports of myriad variations in the cyclometalating ligand.[3b,4d,8] Importantly, the replacement of one CH group in the pyridyl fragment of phenylpyridine by an electronegative nitrogen atom (giving the phenyl pyrazine analogue) has been reported to significantly decrease the LUMO energy level while the HOMO (located over the phenyl group) remains energetically unaltered, in particular in neutral acac complexes such as $[Ir(ppy)_2(acac)]$.[3b] Increasing the π-conjugation by adding an aromatic ring (to give phenyl quinoxaline) will further decrease the band gap and red-shift the $^3\pi-\pi^*$ and ^{3}MLCT emission (Figure 1). To exploit this bathochromic shift of emission,

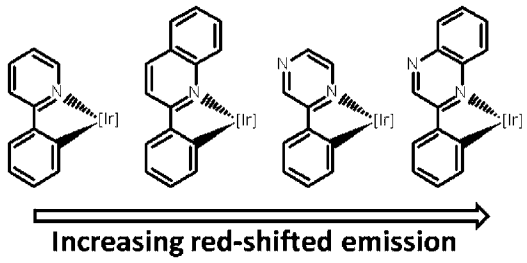

Figure 1. Structures of phenylpyridine, phenylquinoline, phenylpyrazine, and phenylquinoxaline based complexes showing increasing red-shifted emission.

there have been several reports of 2,3-disubstituted quinoxaline derivatives as cyclometalating ligands with various ancillary ligands.[9] In addition, we have previously reported the synthesis and optical properties of amido-substituted phenylquinoline complexes as cyclometalating ligands[10] and substituted hydroxyquinoxalinato complexes as ancillary ligands.[11] It is noteworthy that many applications of solid-state devices require

Received: August 24, 2012
Published: December 27, 2012

   dx.doi.org/10.1021/ic301853t | *Inorg. Chem.* 2013, 52, 448−456

Scheme 1. Synthetic Route to Ligands LH^n, Ir(III) Dimers $[(L^n)_2Ir(\mu\text{-}Cl)_2Ir(L^n)_2]$, and Complexes $[Ir(L^3)_2(bpy)]PF_6$ and $[Ir(L^n)_2(Diobpy)]PF_6$ (n = 1−4)

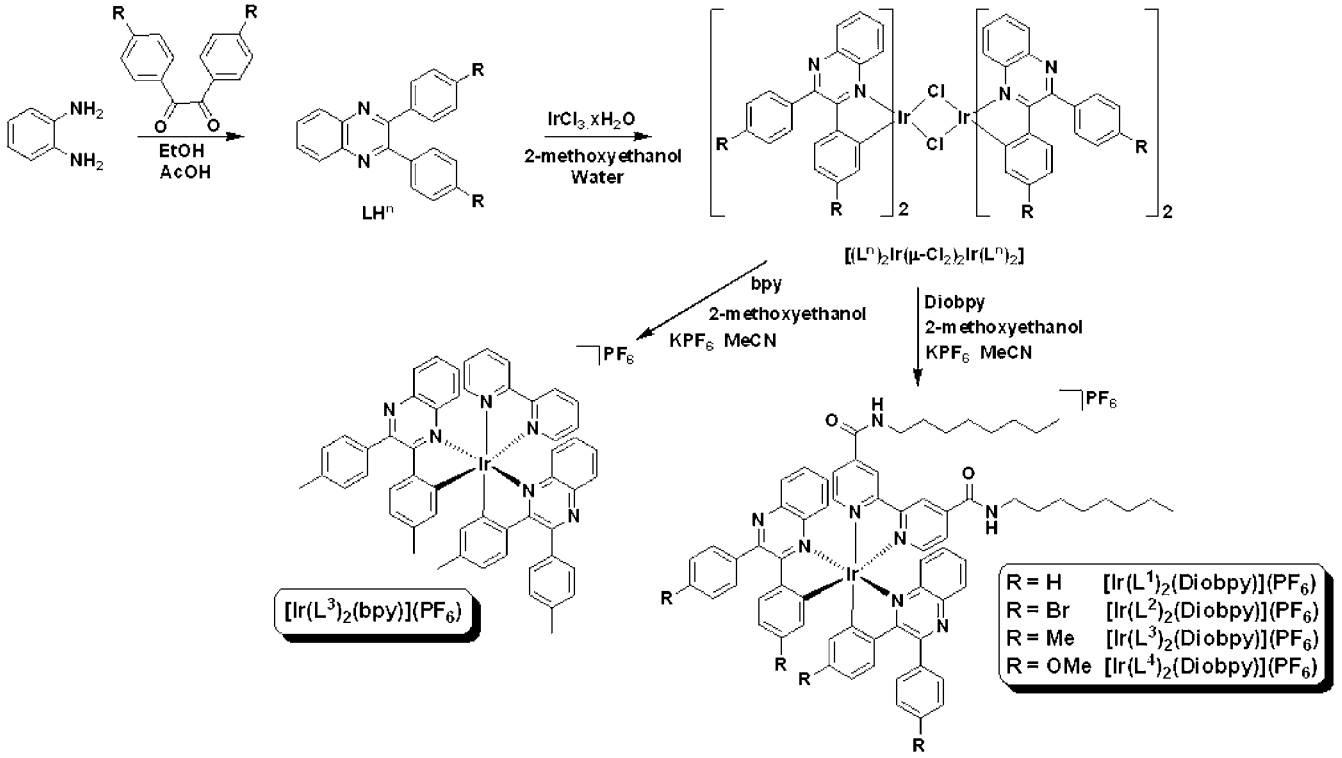

the formation of good quality thin films from the light-emitting component. This is often achieved via vapor deposition or from solutions with the use of alkyl chains on the periphery of the ligand architectures, since these prevent aggregation of complexes.

Following consideration of a number of these design criteria, a class of iridium(III) complexes have been developed, incorporating a range of cyclometalated 2,3-disubstituted quinoxaline ligands, wherein the electronic nature of the aromatic substituent is varied. The ancillary 2,2′-bipyridine ligand has also been functionalized with alkyl amide groups in the 4,4′-positions (which has also been shown to red-shift the absorption of, in particular, ruthenium(II) complexes, via attenuation of ^{1}MLCT transitions),[12] which should aid with solubility and be well suited to film formation and future applicability. This Article presents the syntheses and structural and spectroscopic, including photophysical, characterization of the complexes, together with detailed theoretical studies revealing a class of emissive complexes with tunable electronic properties.

RESULTS AND DISCUSSION

Synthesis and Characterization of the Ligands and Complexes. It is noteworthy that many of the literature reports on functionalized quinoxaline compounds describe biological activities behaving as anticancer,[13] antiviral,[14] antibacterial,[15] and activity as kinase inhibitors.[16] In addition to medicinal applications, quinoxaline derivatives have also found applications as dyes[17] and as components of light emitting diodes (LEDs).[18] For our purposes, the cyclometalating quinoxaline, ligands $\mathbf{LH^n}$ (n = 1−4), were prepared by a simple condensation reaction of 1,2-phenylenediamine with the appropriate diketone in hot ethanol with catalytic acetic acid (Scheme 1). The characterization data were consistent with the published results for these compounds.[19] The ancillary 4,4′-dioctylamido-2,2′-bipyridine (Diobpy) ligand was prepared as previously reported.[12a] The precursor iridium chlorobridged dimers $[(L^n)_2Ir(\mu\text{-}Cl)_2Ir(L^n)_2]$ were synthesized according to established literature conditions for bridged-chloride dimers of this type and used without further purification.[20] Each of the $[(L^n)_2Ir(\mu\text{-}Cl)_2Ir(L^n)_2]$ dimeric compounds readily reacted with 4,4′-dioctylamido-2,2′-bipyridine (Diobpy) in 2-methoxyethanol; workup and counteranion exchange yielded the crude monometallic complexes as $\mathbf{[Ir(L^n)_2(Diobpy)]PF_6}$ (Scheme 1). For comparison, the analogous 2,2′-bipyridine complex $\mathbf{[Ir(L^3)_2(bpy)]PF_6}$ was similarly prepared. Further purification of each complex was achieved using column chromatography (silica). After elution of unreacted starting materials with CH_2Cl_2, the product was eluted as the first band (appearing red) with CH_2Cl_2/MeOH (9:1) giving the complexes as red powders, in good yields of >77%. The resultant complexes are soluble in a range of common organic solvents and were characterized in the solution state using ^{1}H NMR, $^{13}C\{^1H\}$ NMR, IR, UV−vis, and luminescence spectroscopies, and cyclic voltammetry. Additional analysis was provided through X-ray crystallographic studies, ES mass spectrometry (including HR), which revealed the parent cations $[M - PF_6]^+$ for each complex, and elemental analysis.

X-ray Crystallography. Single crystals suitable for X-ray diffraction studies were isolated using vapor diffusion of Et_2O into $CHCl_3$ or MeCN solutions of the complexes $\mathbf{[Ir(L^3)_2(Diobpy)]PF_6}$ and $\mathbf{[Ir(L^3)_2(bpy)]PF_6}$ over a period of 48 h at room temperature. The parameters associated with the data collection are presented in the Supporting Information

dx.doi.org/10.1021/ic301853t | Inorg. Chem. 2013, 52, 448−456

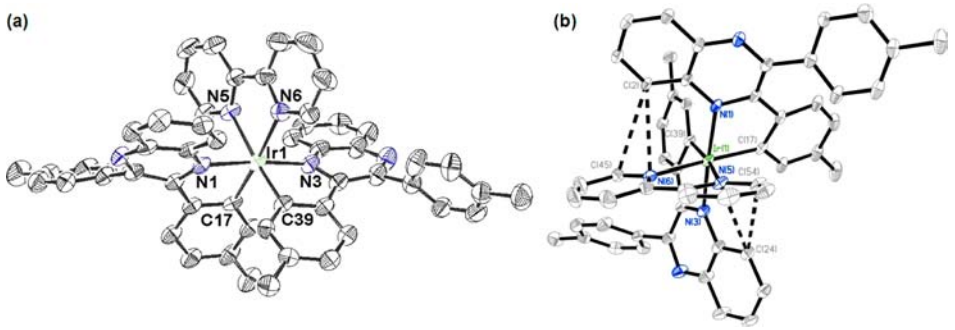

Figure 2. (a) Ortep representation of $[\mathbf{Ir(L^3)_2(bpy)}]^+$ (50% probability ellipsoids, solvent molecules, PF_6^- anion, and hydrogen atoms have been omitted for clarity) and (b) representation showing nonbonding contact interactions between chelating ligands.

(Table S1) with selected bond lengths and angles (principally involving the coordination sphere) shown in Table S2.

The structures obtained for the two complexes $[\mathbf{Ir(L^3)_2(Diobpy)}]\mathbf{PF_6}$ (Figure S1, SI) and $[\mathbf{Ir(L^3)_2(bpy)}]\mathbf{PF_6}$ (Figure 2a) confirmed the suggested formulations from solution state spectroscopic analyses and, even given the disorder along the alkyl chains of $[\mathbf{Ir(L^3)_2(Diobpy)}]\mathbf{PF_6}$, show that the Ir(III) ion in both complexes is octahedrally coordinated by the three chelating ligands (Tables S1 and S2, SI). The diimine always coordinates *trans* to the cyclometalated rings, therefore retaining the *cis*-C,C and *trans*-N,N chelating disposition of the original chloro-bridged dimer, as reported in related examples.[21] Bond lengths and angles for both complexes are consistent with the only structurally characterized Ir quinoxaline diimine complex $[Ir(dpbq)_2(bpy)]^+$ (Hdpbq =2,3-diphenyl benzo[*g*]quinoxaline) {Ir−N1 2.062(6) Å; Ir−N3 2.076(5) Å; Ir−C1 1.992(7) Å; N1−Ir−N3 173.7(2)°}[9n] as well as related neutral quinoxaline complexes.[3b,9d,u]

For both complexes, the uncoordinated and cyclometalated tolyl groups are not coplanar with $[\mathbf{Ir(L^3)_2(bpy)}]\mathbf{PF_6}$ showing twisting angles of 59.2° and 72.6° for each L^3, respectively. In addition, as with $[Ir(dpbq)_2(bpy)]^+$,[9n] there is a distortion within the quinoxaline moiety caused by steric interactions between the chelating ligands (Figure 2b). Most of the interligand C···C and C···N nonbonding contact distances (Table S2) are shorter than 3.4 Å (i.e., the sum of the van der Waals radii of the atoms). This results in the tolyl groups showing deformation angles of 10.10−14.71° with respect to the phenazine fragment of the quinoxaline moiety.

The bond lengths and angles of both $[\mathbf{Ir(L^3)_2(Diobpy)}]\mathbf{PF_6}$ and $[\mathbf{Ir(L^3)_2(bpy)}]\mathbf{PF_6}$ were compared with the optimized values calculated from density functional theory studies (see DFT Studies section and Table S2, SI). In general, a reasonable agreement is obtained between the theoretical and experimentally observed bond lengths, although some small differences are found. The calculated $Ir-N_{bipyridine}$ bond lengths are, respectively, 0.038 and 0.054 Å longer than the experimental values for $[\mathbf{Ir(L^3)_2(bpy)}]\mathbf{PF_6}$ of Ir−N(5) (2.186 Å) and Ir−N(6) (2.169 Å). In the case of the cyclometalated bonds, the calculated value is 1.997 Å and comparable to Ir−C(39) 1.999(5) Å for $[\mathbf{Ir(L^3)_2(bpy)}]\mathbf{PF_6}$, but 0.010 Å longer than the value obtained by X-ray crystallography for Ir−C(17); the $Ir-N_{quinoxline}$ bonds are similar, where the calculated values are 0.023 and 0.016 Å longer. Again, there are C···C and C···N interactions between the ligands, although the contact distances are larger. This results in lower deformation angles compared to experimental values for $[\mathbf{Ir(L^3)_2(bpy)}]^+$ of 8.88−13.09° with respect to the phenazine fragment of the quinoxaline moiety, with the largest distortions on the cyclometalating tolyl groups.

Density Functional Theory (DFT) Studies. DFT calculations (computed using the B3PW91 hybrid functional) were performed to assess the frontier orbitals and provide qualitative descriptions of the HOMO (highest occupied molecular orbital) and LUMO (lowest unoccupied molecular orbital) energy levels.

For the phenyl-substituted quinoxaline complexes described here the energy levels of both the HOMO and LUMO are sufficiently different ($\Delta E > 0.2$ eV) from the other MOs to be considered independent. In each case the HOMO of $[\mathbf{Ir(L^n)_2(Diobpy)}]^+$ is located on the metal 5d(Ir) center and the cyclometalated phenylquinoxaline (Figure 3). For $[\mathbf{Ir(L^1)_2(Diobpy)}]^+$ and $[\mathbf{Ir(L^3)_2(Diobpy)}]^+$ there is little or no contribution from the uncoordinated substituted phenyl moieties to the HOMO coverage. However, for $[\mathbf{Ir(L^2)_2(Diobpy)}]^+$ and $[\mathbf{Ir(L^4)_2(Diobpy)}]^+$ there is contribution with one cyclometalated ligand (L^n 1) showing greater coverage that the second ligand (L^n 2) (Figure 3, Table 1).

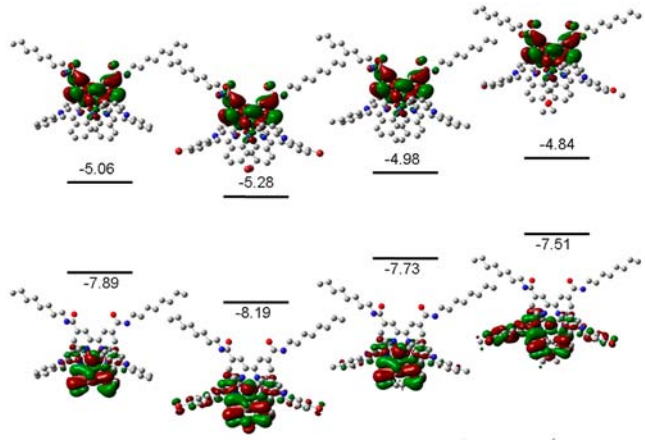

Figure 3. Graphical representation of the frontier orbitals of $[\mathbf{Ir(L^n)_2(Diobpy)}]^+$ (n = 1−4 left to right): bottom, HOMO; top, LUMO.

The nature of the pendant R-group imparts an influence on the overall energy level of the HOMO. This is unsurprising, given that one of the R-groups is bound directly to a cyclometalating phenyl moiety on each ligand L^n. Of the complexes $[\mathbf{Ir(L^n)_2(Diobpy)}]^+$ (n = 1−4), the electron withdrawing *para*-Br ligands of $[\mathbf{Ir(L^2)_2(Diobpy)}]^+$ induced the lowest HOMO energy level (E = −8.19 eV), whereas the

dx.doi.org/10.1021/ic301853t | *Inorg. Chem.* 2013, 52, 448−456

Table 1. Percentage Distribution of HOMO and LUMO in $[Ir(L^n)_2(Diobpy)]^+$ (n = 1−4) and $[Ir(L^3)_2(bpy)]^+$

	$[Ir(L^1)_2(Diobpy)]^+$		$[Ir(L^2)_2(Diobpy)]^+$		$[Ir(L^3)_2(Diobpy)]^+$		$[Ir(L^4)_2(Diobpy)]^+$		$[Ir(L^3)_2(bpy)]^+$	
	HOMO	LUMO	HOMO	LUMO	HOMO	LUMO	HOMO	LUMO	HOMO	LUMO
Ir	42.4	3.3	28.8	3.3	38.4	3.4	11.4	3.5	37.6	2.8
bpy	3.3	93.2	2.2	93.3	3.0	93.2	1.0	93.3	2.9	93.9
L^n 1	26.5	1.7	37.9	1.7	30.6	1.7	61.7	1.6	27.9	1.7
L^n 2	27.9	1.8	31.1	1.7	28.1	1.7	25.9	1.6	31.6	1.6

Table 2. Absorption and Electrochemical Properties of $[Ir(L^n)_2(Diobpy)]PF_6$ (n = 1−4) and $[Ir(L^3)_2(bpy)]PF_6$

complex	λ_{max}/nm (ε/M^{-1} cm^{-1})[a]	E_{ox}/V[b]	HOMO/eV[c]	$E_{bandgap}$/eV[d]	LUMO/eV[e]
$[Ir(L^1)_2(Diobpy)]PF_6$	294 (60 400), 386 (28 600), 447 (10 000)	2.00	−6.35	2.12	−4.23
$[Ir(L^2)_2(Diobpy)]PF_6$	293 (41 600), 386 (17 200), 447 (6000)	2.02	−6.37	2.10	−4.27
$[Ir(L^3)_2(Diobpy)]PF_6$	296 (40 400), 388 (21 600), 466 (5900)	1.99	−6.34	2.12	−4.22
$[Ir(L^4)_2(Diobpy)]PF_6$	305 (44 500), 398 (19 300), 415 (19 100), 458 (11 300)	1.97	−6.32	2.10	−4.22
$[Ir(L^3)_2(bpy)]PF_6$	298 (39 800), 388 (19 600), 471 (4900)	1.52	−5.87	2.09	−3.78

[a]Absorption spectra measured in MeCN solutions (5×10^{-5} mol dm^{-3}). [b]Oxidation potentials measured in CH_2Cl_2 solutions at 200 mV s^{-1} with 0.1 M $[NBu_4][PF_6]$ as supporting electrolyte calibrated with Fc/Fc^+. [c]The HOMO energy level was calculated using the equation $-E_{HOMO}$ (eV) = $E_{ox} - E_{Fc/Fc^+} + 4.8$. [d]$E_{bandgap}$ was determined from the absorption edge of the iridium complexes. [e]The LUMO energy level was calculated using the equation E_{LUMO} (eV) = $E_{HOMO} + E_{bandgap}$.

complex of the electron donating *para*-OMe groups has the highest (E = −7.51 eV). The LUMO energies also reflect the variation of pendant R-group (*para*-Br E_{LUMO} = −5.28 eV; *para*-OMe E_{LUMO} = −4.84 eV). This calculated data suggests that variation of the *para*-substituent can lead to a degree of tunable optical properties within this series of complexes. Unlike our previously reported substituted phenylquinoline[10] and quinoxalinato[11] Ir(III) complexes, the calculated HOMO−LUMO band gaps do show a significant variance (2.67−2.91 eV). The LUMOs for all complexes are almost entirely delocalized over the 2,2′-bipyridine ligand. Population analyses revealed that the distribution of the frontier orbitals over the various ligands and metal varies substantially for the HOMOs of $[Ir(L^n)_2(Diobpy)]^+$ (n = 1−4) (HOMO: 11.4−42.4% Ir; 1.0−3.3% bpy; 26.5−61.7% L^n 1; 25.9−31.1% L^n 2) but for the LUMOs is essentially identical (LUMO: 3.3−3.5% Ir; 93.2−93.3% bpy; 1.6−1.7% L^n 1; 1.6−1.8% L^n 2) (Table 1).

The bpy complex $[Ir(L^3)_2(bpy)]^+$ (E_{HOMO} −7.76 eV, E_{LUMO} −4.92 eV) showed no significant difference from the Diobpy analogue. The HOMO is located over the iridium center (37.6%) and the cyclometalating ligands (27.9 and 31.6%) with little or no contribution from the uncoordinated phenyl ring (Figure S2). The LUMO is again almost entirely delocalized over the 2,2′-bipyridine ligand (93.9%).

Electrochemical Studies. The electrochemical characteristics of the four $[Ir(L^n)_2(Diobpy)]PF_6$ (n = 1−4) complexes and $[Ir(L^3)_2(bpy)]PF_6$ were studied in deoxygenated CH_2Cl_2. The HOMO energy levels (E_{HOMO}) can be determined from the ionization potential of the first oxidation ($Ir^{3+/4+}$) by direct correlation with the redox couple of $FeCp_2^{0/1+}$. The cyclic voltammograms, measured at a platinum disc electrode (scan rate v = 200 mV s^{-1}, 1×10^{-3} M solutions, 0.1 M $[NBu_4][PF_6]$ as a supporting electrolyte), each showed one nonfully reversible oxidation (Table 2), over a range very close to the edge of the solvent window (+1.97 to +2.02 V), for the 4,4′-dioctylamido-2,2′-bipyridine complexes. The extent of the irreversibility can be ascribed to the varying contribution of the cyclometalating ligands to the electron density of the HOMO,[22] which in this case is calculated to be 54−87%. The subtle differences in potential are probably due to the *para*-phenyl substituent on the cyclometalating ligand having a small influence on the electron density at iridium. The E_{HOMO} values were determined using the relevant equations,[23] and the resultant values (Table 2) fall in the narrow range −6.37 to −6.32 eV. The electronic nature of the bipyridine ligand has a larger effect on the oxidation potential: removal of the electron withdrawing alkylamido groups in the 4,4′-positions of $[Ir(L^3)_2(Diobpy)]PF_6$ to give $[Ir(L^3)_2(bpy)]PF_6$ results in a lowering of the $Ir^{3+/4+}$ oxidation potential by +0.47 to +1.52 V, and a resultant E_{HOMO} value of −5.87 eV. This is contradictory to DFT calculations which essentially show no difference between the location and energy levels for the HOMO of both complexes. Each complex also showed one or two partially reversible or irreversible reduction waves, assigned to ligand-centered processes involving both the bipyridine and quinoxaline ligands.

Electronic Properties of the Complexes. The cationic complexes each absorb in the UV−vis regions (Table 2, Figure 4) with variations in the positioning of the lowest energy shoulder absorption. Ligand-centered transitions clearly dominate at shorter wavelengths while the presence of charge transfer (CT) bands accounts for the visible absorption characteristics with large absorption coefficients (~10^4 M^{-1} cm^{-1}). With reference to the DFT calculations, it is clear that both metal-to-ligand CT (MLCT) and ligand-to-ligand CT (LLCT) transitions can contribute to the low-energy profiles of the absorption spectra, and it should be noted that iridium-mediated spin−orbit coupling can faciliate some ^{3}MLCT/^{3}LLCT character as well. Since the HOMO possesses significant coverage of the substituted quinoxaline ligands it is likely that the nature of the substituent influences the absorption characteristics, albeit subtly.

Nonrelativistic TD-DFT calculations (SI) in simulated MeCN on $[Ir(L^3)_2(bpy)]^+$ support the assignment of these bands as having substantial MLCT and LLCT character. The lowest energy absorption with significant intensity consists of excitation from the HOMO (metal + quinoxaline) into π^* orbitals on both bpy and quinoxaline. This is predicted to lie at 501 nm (oscillator strength = 0.05 au), and so coincides reasonably closely with the lowest energy peak seen in Figure 4. A set of stronger bands centered around 410 nm (424 nm, 0.12 au; 408 nm, 0.10 au; 397 nm, 0.15 au) are also predicted, again

dx.doi.org/10.1021/ic301853t | Inorg. Chem. 2013, 52, 448−456

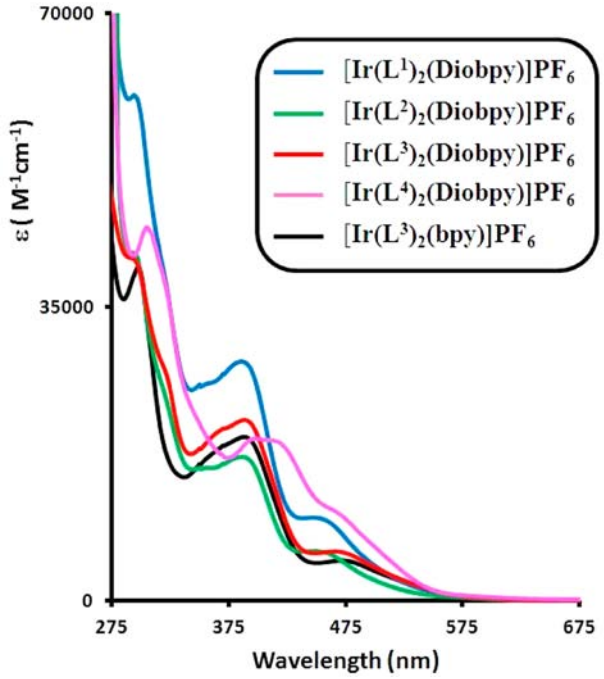

Figure 4. UV−vis spectra of $[Ir(L^n)_2(Diobpy)]PF_6$ (n = 1−4) and $[Ir(L^3)_2(bpy)]PF_6$ in MeCN solutions (5×10^{-5} M).

in good agreement with Figure 4. These bands consist of varying combinations of metal and L^3 π orbitals excited into L^3 π^* orbitals, but have no contribution from the bpy π^* orbitals, suggesting MLCT and IL contributions. The largest intensity bands are shown in Table 3 (with the dominant excitation in bold), and a full breakdown of all orbitals involved, with a predicted absorption spectrum, is shown in the Supporting Information (Table S3 and Figure S3).

Table 3. Calculated Excitation Wavelengths for $[Ir(L^3)_2(bpy)]^+$ from Scalar DFT Studies Showing the Dominant Contribution to Each Transition in Bold

λ (nm)[a]	f	character
501	0.0491	**HOMO → LUMO + 1**
		HOMO → LUMO + 2
424	0.1218	HOMO − 3 → LUMO
		HOMO − 1 → LUMO
408	0.1015	HOMO − 4 → LUMO
		HOMO − 2 → LUMO
		HOMO − 1 → LUMO + 1
397	0.1487	**HOMO − 3 → LUMO**
		HOMO − 2 → LUMO + 1
		HOMO − 1 → LUMO

[a]Excitation wavelength.

The complexes are visibly luminescent in a variety of solvents (Tables 4 and 5) with corresponding lifetime values (τ) in the range 288−420 ns, and modest quantum yields (Φ) which are in line with related species. Comparison of the excitation spectra for the complexes $[Ir(L^3)_2(Diobpy)]PF_6$ and $[Ir(L^3)_2(bpy)]PF_6$ (Figure 5) highlight the differences in the visible part (400−550 nm) of the spectral profile through simple substitution of the bipyridine ligand. The variation of emission wavelengths in MeCN reveals the subtle, but effective, influence of the remote aryl substituents of the cyclometalated

Table 4. Photophysical Properties of $[Ir(L^n)_2(Diobpy)]PF_6$ (n = 1−4) and $[Ir(L^3)_2(bpy)]PF_6$

complex	λ_{em}/nm[a,b]	τ/ns[a]	Φ_{em}[a]	$k_r/s^{-1} \times 10^4$	$k_{nr}/s^{-1} \times 10^6$
$[Ir(L^1)_2(Diobpy)]PF_6$	628 (686)	359	0.024	6.7	2.7
$[Ir(L^2)_2(Diobpy)]PF_6$	618 (699)	420	0.018	4.3	2.3
$[Ir(L^3)_2(Diobpy)]PF_6$	631 (677)	317	0.027	8.5	3.1
$[Ir(L^4)_2(Diobpy)]PF_6$	636 (699)	298	0.022	7.4	3.3
$[Ir(L^3)_2(bpy)]PF_6$	633 (688)	288	0.021	7.3	3.4

[a]Recorded in aerated MeCN (λ_{ex} = 425 nm). [b]Values in parentheses are the emission maxima obtained on solid samples.

quinoxaline ligands, with electron donating groups (Me and OMe; L^3 and L^4, respectively) shifting λ_{em} to lower energy. The quinoxaline based complexes here show emission maxima ca. 3000 cm^{-1} lower energy than the analogous phenylpyridine complex $[Ir(ppy)_2(bpy)]^+$.[7b,c] A graphical plot (Figure S4, SI) of E versus k_{nr} revealed a good linear correlation, suggesting that the series of 4,4′-dioctylamido-2,2′-bipyridine complexes obey the energy gap law.

The expected sensitivity of the emission wavelengths to different solvent polarities confirmed that the excited states are characterized with significant CT character, wherein more polar solvents bathochromically shift λ_{em}. The complexes also showed a somewhat unusual solvent-dependent variance in emission lifetime. From the related time-resolved deoxygenated measurements it was possible to approximate the rate of quenching by oxygen, $k_q(O_2)$, for a given solvent. These calculated values revealed that the rate of quenching in chloroform and toluene ($\sim 2 \times 10^6$ s^{-1}) was an order of magnitude greater than in acetonitrile or dimethyl sulfoxide ($\sim 8 \times 10^5$ s^{-1}). Typically, luminescent complexes of the type $[Ru(N^\wedge N)_3]^{2+}$ and $[Ir(ppy)_2(N^\wedge N)]^+$ possess a lower rate of quenching by oxygen in lower polarity media.[24] However, the quinoxaline-derived complexes here do not adhere to that precedent.

Measurements obtained on solid films deposited from the slow evaporation of solvent revealed broad, bathochromically shifted emission maxima. In all cases, obtained lifetime decay profiles were sensitive to the wavelength of detection and best fitted to two exponential components (Table S4, SI). This suggests that (at least) two emitting species coexist in the solid state and contribute to the emission profile, presumably due to packing influences, the differences in the local environment of the luminophore, and therefore difference in quenching (cf. comments regarding O_2 sensitivity above) associated with those environments. However, the dominant contribution in each case was the retention of a long-lived species and is therefore consistent with a phosphorescence and the observations in solution. The luminescent lifetimes of these species were generally longer than those in solution for the octylamido appended complexes.

Nonrelativistic TD-DFT calculations on $[Ir(L^3)_2(bpy)]^+$ in MeCN again support these experimental observations. The lowest energy triplet state is found to lie 2.05 eV, or 604 nm above the ground state, at the optimal geometry of the triplet state, in good agreement with the experimental value (633 nm = 1.96 eV). This transition is dominated by the HOMO and LUMO (76%), and hence, we can surmise that the emission of

dx.doi.org/10.1021/ic301853t | Inorg. Chem. 2013, 52, 448−456

Table 5. Photophysical Properties of $[Ir(L^n)_2(Diobpy)]PF_6$ (n = 1−4) and $[Ir(L^3)_2(bpy)]PF_6$ in Various Air-Equilibrated Solvents

	λ_{em}/nm (τ/ns)			
complex	toluene	$CHCl_3$	MeCN	DMSO
$[Ir(L^1)_2(Diobpy)]PF_6$	619 (454)	622 (511)	628 (359)	634 (939)
$[Ir(L^2)_2(Diobpy)]PF_6$	612 (435)	615 (591)	618 (420)	622 (992)
$[Ir(L^3)_2(Diobpy)]PF_6$	622 (389)	628 (459)	631 (317)	639 (744)
$[Ir(L^4)_2(Diobpy)]PF_6$	628 (424)	634 (504)	636 (298)	642 (788)
$[Ir(L^3)_2(bpy)]PF_6$	632 (336)	632 (432)	633 (288)	640 (636)

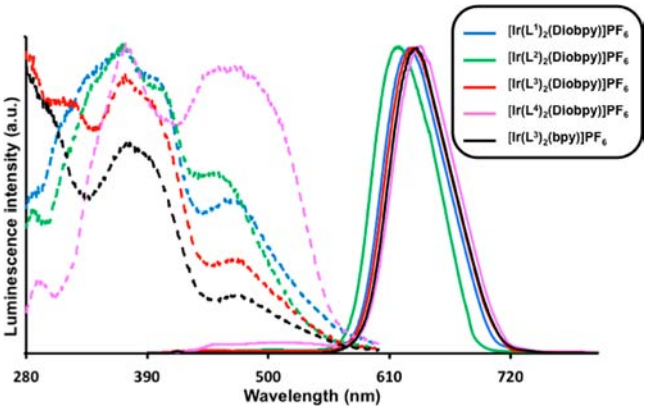

Figure 5. Excitation (– – –) and emission (—) spectra of $[Ir(L^n)_2(Diobpy)]PF_6$ (n = 1−4) and $[Ir(L^3)_2(bpy)]PF_6$ recorded in MeCN solutions.

this complex (and its analogues in the series) is indeed of ^{3}MLCT and/or ^{3}LLCT character.

CONCLUSIONS

Aryl disubstituted quinoxaline-type chromophores have been cyclometalated to iridium(III) forming mixed ligand species of the general form $[Ir(L^n)_2(bpy)]PF_6$ where the ancillary bipyridine can incorporate octyl chains, facilitating excellent solubility properties upon the complexes. The complexes have been comprehensively characterized through a variety of experimental and theoretical studies. The substituents impart a subtle modulation upon the electronic character of the complexes, which generally possess excellent visible region molar absorption coefficients. In the excited state this perturbation manifests itself in varied emission wavelengths and lifetimes, which are best described by a significant ^{3}MLCT character; this luminescence was also sensitive to the nature of the solvent. DFT calculations confirm that orbital energies can be tuned by variation of substituent, and also support the assignment of lowest energy absorption and emission spectra as mixed ^{3}MLCT/^{3}LLCT character. Future work will investigate the potential application of these complexes in electroluminescent devices with a primary focus upon the quality of film formation.

EXPERIMENTAL DETAILS

All reactions were performed with the use of vacuum line and Schlenk techniques. Reagents were commercial grade and were used without further purification. ^{1}H and ^{13}C{^{1}H} NMR spectra were recorded on an NMR-FT Bruker 400 MHz or Joel Eclipse 300 MHz spectrometer and recorded in $CDCl_3$. ^{1}H and ^{13}C{^{1}H} NMR chemical shifts (δ) were determined relative to internal tetramethylsilane, $Si(CH_3)_4$, and are given in ppm. Low-resolution mass spectra were obtained by the staff at Cardiff University. High-resolution mass spectra were carried out at the EPSRC National Mass Spectrometry Service at Swansea University. UV−vis studies were performed on a Jasco V-570 spectrophotometer in MeCN solutions (5×10^{-5} M). IR spectra were recorded on a Thermo Scientific Nicolet iS5 spectrometer fitted with an iD3 ATR attachment. Photophysical data were obtained on a JobinYvon−Horiba Fluorolog spectrometer fitted with a JY TBX picoseconds photodetection module. Emission spectra were uncorrected, and excitation spectra were instrument corrected. The pulsed source was a Nano-LED configured for 372 nm output operating at 500 kHz. Luminescence lifetime profiles were obtained using the JobinYvon−Horiba FluoroHub single photon counting module and the data fits yielded the lifetime values using the provided DAS6 deconvolution software. Quantum yield measurements were obtained on aerated MeCN solutions of the complexes, using $[Ru(bpy)_3](PF_6)_2$ in aerated MeCN as a standard (Φ_{em} = 0.016).[25] Electrochemical studies were carried out using a Parstat 2273 potentiostat in conjunction with a three-electrode cell. The auxiliary electrode was a platinum wire and the working electrode a platinum (1.0 mm diameter) disc. The reference was a silver wire separated from the test solution by a fine porosity frit and an agar bridge saturated with KCl. Solutions (10 mL CH_2Cl_2) were 1.0×10^{-3} mol dm^{-3} in the test compound and 0.1 mol dm^{-3} in $[NBu^n_4][PF_6]$ as the supporting electrolyte. Under these conditions, $E^{0\prime}$ for the one-electron oxidation of $[Fe(\eta\text{-}C_5H_5)_2]$, added to the test solutions as an internal calibrant, is 0.46 V.[26] Unless specified, all electrochemical values are at υ = 200 mV s^{-1}. Microanalyses were performed by Medac Ltd., U.K.

Data Collection and Processing. Diffraction data for $[Ir(L^3)_2(bpy)]PF_6$, and $[Ir(L^3)_2(Diobpy)]PF_6$ were collected on a Nonius KappaCCD using graphite-monochromated Mo Kα radiation (λ = 0.710 73 Å) at 150 K. Software package Apex 2 (v2.1) was used for the data integration, scaling, and absorption correction. CCDC reference numbers 890952 and 890953 contain the supplementary crystallographic data for this paper. These data can be obtained free of charge from the Cambridge Crystallographic Data Centre via www.ccdc.cam.ac.uk/data_request/cif.

Structure Analysis and Refinement. The structure was solved by direct methods using SHELXS-97 and was completed by iterative cycles of ΔF-syntheses and full-matrix least-squares refinement. All non-H atoms were refined anisotropically, and difference Fourier syntheses were employed in positioning idealized hydrogen atoms and were allowed to ride on their parent C-atoms. All refinements were against F^2 and used SHELX-97.[27]

DFT Studies. Nonrelativistic calculations were performed on the Gaussian 03 program.[28] Geometry optimizations were carried out without constraints using the B3PW91 functional. The LANL2DZ[29] basis set was used for the Ir centers, and was invoked with pseudopotentials for the core electrons, a 6-31G(d,p)[30] basis set for all coordinating atoms with a 6-31G[31] basis set for all remaining atoms. All optimizations were followed by frequency calculations to ascertain the nature of the stationary point (minimum or saddle point). TD-DFT studies were performed using the functional, but with 6-31G(d) on all nonmetal atoms, and also included a simulated MeCN environment using the polarized continuum model (PCM) approach.[32] For prediction of absorption spectra, the geometry used to calculate orbital and other properties was used without modification. For prediction of emission, however, the triplet state

dx.doi.org/10.1021/ic301853t | Inorg. Chem. 2013, 52, 448−456

was allowed to relax to its optimal geometry using unrestricted B3PW91 in the gas phase, prior to solvated TD-DFT.

Synthesis. The cyclometalating ligands **LH^n** (n = 1−4) were prepared according to the literature procedures.[33] 4,4′-Dioctylamido-2,2′-bipyridine (Diobpy) was prepared as previously reported.[12a]

General Procedure for the Synthesis of Ir(III) μ-Chloro-bridged Dimers. Cyclometalated Ir(III) μ-chlorobridged dimers $[(C^N)_2Ir(\mu\text{-}Cl)_2Ir(C^N)_2]$ were synthesized according to the Nonoyama route.[20] $IrCl_3{\cdot}xH_2O$ (0.200 g, 0.68 mmol) and **LH^n** (2.5 equiv) in 2-methoxyethanol (9 mL) and distilled water (3 mL) were heated at 120 °C for 48 h. The mixture was allowed to cool, and the product precipitated on addition of distilled water (30 mL). The red solids were collected by filtration, washed with distilled water, and dried in an oven. The Ir(III) dimers were used in subsequent reactions without purification or characterization.

[Ir(L^1)$_2$(Diobpy)]PF$_6$. $[(L^1)_2Ir(\mu\text{-}Cl)_2Ir(L^1)_2]$ (0.085 g, 0.054 mmol) and 4,4′-dioctylamido-2,2′-bipyridine (0.053 g, 0.114 mmol) were heated at 120 °C in 2-methoxyethanol (10 mL) for 16 h. The solvent was then removed *in vacuo* and the crude product dissolved in MeCN (4 mL). An excess of KPF_6 (1.10 g, 5.976 mmol) in distilled water (2 mL) was added and the solution stirred for 10 min. Distilled water (30 mL) was then added and the product extracted with CH_2Cl_2 (2 × 20 mL). The combined organic phases were washed with water (30 mL) and brine (30 mL) before being dried over $MgSO_4$. The solution was filtered and the solvent removed *in vacuo*. The product was purified by column chromatography (silica, CH_2Cl_2) and was eluted as the first red fraction with CH_2Cl_2/MeOH (9:1). The solvent was lowered in volume (to ca. 3 mL) and the product precipitated by the slow addition of Et_2O (25 mL), filtered, and dried *in vacuo*. Yield = 0.128 g, 87%. ^{1}H NMR (400 MHz, $CDCl_3$) δ_H = 8.61 (2H, d, $^3J_{HH}$ = 5.9 Hz), 8.49 (2H, br s), 8.13 (2H, d, $^3J_{HH}$ = 5.8 Hz), 7.96 (2H, d, $^3J_{HH}$ = 7.9 Hz), 7.75−7.71 (4H, br d), 7.60−7.55 (4H, m), 7.52 (2H, app. t {coincident dd}, $^3J_{HH}$ = 7.4 Hz), 7.45 (2H, br), 7.18−7.06 (6H, m), 6.72 (2H, app. t, $^3J_{HH}$ = 7.9 Hz), 6.66 (2H, app. t, $^3J_{HH}$ = 7.9 Hz), 6.40 (2H, d, $^3J_{HH}$ = 7.9 Hz), 3.47−3.38 (4H, m), 1.61−1.52 (4H, m), 1.27−1.05 (20H, m), 0.77 (6H, t, $^3J_{HH}$ = 7.3 Hz) ppm. ^{13}C{^{1}H} NMR (75 MHz, $CDCl_3$) δ_C = 163.1, 162.8, 155.9, 154.0, 152.0, 148.3, 146.0, 143.9, 140.6, 140.0, 139.3, 134.6, 131.9, 131.8, 131.3, 130.9, 130.6, 130.4, 129.5, 128.9, 127.5, 123.4, 122.9, 121.7, 40.9, 31.9, 29.6, 29.2, 29.0, 27.0, 22.7, 14.1 ppm. UV−vis (MeCN): λ_{max} (ε/dm^3 mol^{-1} cm^{-1}) 294 (60 350), 386 (28 550), 447 (9950) nm. IR (ATR): υ(CO) = 1672 cm^{-1}. Anal. Calcd (%) for $C_{68}H_{68}N_8O_2IrPF_6{\cdot}0.5CH_2Cl_2$: C, 58.39, H, 4.94, N, 7.95. Found: C, 58.37, H, 5.13, N, 7.89. ES MS found m/z 1221.5, calculated m/z 1221.5 for $[M - PF_6]^+$. HR MS found m/z 1219.5077, calculated m/z 1219.5066 for $[C_{68}H_{68}N_8O_2{}^{191}Ir]^+$.

[Ir(L^2)$_2$(Diobpy)]PF$_6$. This compound was prepared similarly from $[(L^2)_2Ir(\mu\text{-}Cl)_2Ir(L^2)_2]$ (0.088 g, 0.040 mmol) and 4,4′-dioctylamido-2,2′-bipyridine (0.040 g, 0.086 mmol). Yield 0.108 g (81%). ^{1}H NMR (400 MHz, $CDCl_3$) δ_H = 8.50 (4H, d, $^3J_{HH}$ = 5.7 Hz), 8.12 (2H, d, $^3J_{HH}$ = 5.6 Hz), 7.96 (2H, d, $^3J_{HH}$ = 8.3 Hz), 7.72 (4H, d, $^3J_{HH}$ = 8.5 Hz), 7.67−7.52 (6H, m), 7.13 (2H, app. t, $^3J_{HH}$ = 7.2 Hz), 7.02 (4H, app. t, $^3J_{HH}$ = 9.2 Hz), 6.96 (2H, d, $^3J_{HH}$ = 8.7 Hz), 6.51 (2H, s), 3.48−3.35 (4H, m), 1.60−1.46 (4H, m), 1.29−1.01 (20H, m), 0.75 (6H, t, $^3J_{HH}$ = 7.2 Hz) ppm. ^{13}C{^{1}H} NMR (75 MHz, $CDCl_3$) δ_C = 162.7, 162.1, 155.9, 152.8, 152.7, 148.4, 146.6, 142.7, 140.9, 139.8, 137.6, 136.7, 132.9, 132.8, 131.5, 130.9, 130.6, 130.5, 127.7, 127.3, 126.8, 125.3, 122.8, 122.2, 41.0, 31.9, 29.3, 29.2, 29.0, 27.0, 22.7, 14.2 ppm. UV−vis (MeCN): λ_{max} (ε/dm^3 mol^{-1} cm^{-1}) 293 (41 550), 386 (17 150), 447 (5950) nm. IR (ATR): υ(CO) = 1673 cm^{-1}. Anal. Calcd (%) for $C_{68}H_{64}N_8Br_4O_2IrPF_6$: C, 48.55, H, 3.84, N, 6.66. Found: C, 48.28, H, 3.95, N, 6.52. ES MS found m/z 1537.1, calculated m/z 1537.1 for $[M - PF_6]^+$. HR MS found m/z 1531.1450, calculated m/z 1531.1486 for $[C_{68}H_{64}N_8Br_4O_2{}^{191}Ir]^+$.

[Ir(L^3)$_2$(Diobpy)]PF$_6$. This compound was prepared similarly from $[(L^3)_2Ir(\mu\text{-}Cl)_2Ir(L^3)_2]$ (0.080 g, 0.047 mmol) and 4,4′-dioctylamido-2,2′-bipyridine (0.048 g, 0.103 mmol). Yield 0.104 g (77%). ^{1}H NMR (400 MHz, $CDCl_3$) δ_H = 8.52 (2H, d, $^3J_{HH}$ = 5.7 Hz), 8.41 (2H, br s), 8.08 (2H, d, $^3J_{HH}$ = 5.8 Hz), 7.91 (2H, d, $^3J_{HH}$ = 7.8 Hz), 7.59 (4H, d, $^3J_{HH}$ = 7.8 Hz), 7.48 (2H, app. t, $^3J_{HH}$ = 7.0 Hz), 7.33 (4H, d, $^3J_{HH}$ = 7.9 Hz), 7.11−6.96 (6H, m), 6.56 (2H, d, $^3J_{HH}$ = 8.4 Hz), 6.19 (2H, s), 3.44−3.28 (4H, m), 2.48 (6H, s), 1.49 (6H, s), 1.60−1.46 (4H, m), 1.31−1.09 (20H, m), 0.75 (6H, t, $^3J_{HH}$ = 7.0 Hz) ppm. ^{13}C{^{1}H} NMR (75 MHz, $CDCl_3$) δ_C = 163.3, 162.9, 155.9, 153.9, 152.4, 148.5, 145.9, 142.1, 141.3, 140.6, 140.4, 139.9, 136.6, 135.1, 131.7, 131.5, 130.5, 130.3, 130.1, 128.8, 127.5, 124.1, 123.2, 121.4, 41.0, 31.9, 29.3, 29.2, 29.0, 27.0, 22.7, 21.8, 21.7, 14.2 ppm. UV−vis (MeCN): λ_{max} (ε/dm^3 mol^{-1} cm^{-1}) 296 (40 350), 388 (21 550), 466 (5900) nm. IR (ATR): υ(CO) = 1671 cm^{-1}. Anal. Calcd (%) for $C_{72}H_{76}N_8O_2IrPF_6{\cdot}0.5CH_2Cl_2$: C, 59.44, H, 5.30, N, 7.65. Found: C, 59.50, H, 5.38, N, 7.49. ES MS found m/z 1277.6, calculated m/z 1277.6 for $[M - PF_6]^+$. HR MS found m/z 1275.5695, calculated m/z 1275.5692 for $[C_{72}H_{76}N_8O_2{}^{191}Ir]^+$.

[Ir(L^4)$_2$(Diobpy)]PF$_6$. This compound was prepared similarly from $[(L^4)_2Ir(\mu\text{-}Cl)_2Ir(L^4)_2]$ (0.084 g, 0.046 mmol) and 4,4′-dioctylamido-2,2′-bipyridine (0.045 g, 0.096 mmol). Yield 0.112 g (82%). ^{1}H NMR (400 MHz, $CDCl_3$) δ_H = 8.60 (2H, d, $^3J_{HH}$ = 5.7 Hz), 8.55 (2H, br s), 8.11 (2H, d, $^3J_{HH}$ = 5.6 Hz), 7.87 (2H, d, $^3J_{HH}$ = 6.8 Hz), 7.68 (4H, d, $^3J_{HH}$ = 8.2 Hz), 7.43 (2H, app. t, $^3J_{HH}$ = 7.2 Hz), 7.19 (2H, d, $^3J_{HH}$ = 8.4 Hz), 7.11−6.98 (8H, m), 6.36 (2H, d, $^3J_{HH}$ = 8.6 Hz), 5.87 (2H, s), 3.88 (6H, s), 3.38 (6H, s), 3.36−3.24 (4H, m), 1.60−1.48 (4H, m), 1.28−1.04 (20H, m), 0.75 (6H, t, $^3J_{HH}$ = 6.8 Hz) ppm. ^{13}C{^{1}H} NMR (75 MHz, $CDCl_3$) δ_C = 162.9, 162.7, 161.3, 161.1, 156.0, 154.5, 153.3, 148.6, 145.9, 140.2, 139.7, 136.8, 133.7, 131.8, 131.4, 130.4, 129.9, 127.5, 123.0, 121.6, 119.9, 115.1, 114.9, 108.4, 55.7, 54.9, 41.0, 31.9, 29.3, 29.2, 29.1, 27.0, 22.7, 14.2 ppm. UV−vis (MeCN): λ_{max} (ε/dm^3 mol^{-1} cm^{-1}) 305 (44 500), 398 (19 300), 415 (19 050), 458 (11 250) nm. IR (ATR): υ(CO) = 1672 cm^{-1}. Anal. Calcd (%) for $C_{72}H_{76}N_8O_6IrPF_6{\cdot}0.5CH_2Cl_2$: C, 56.95, H, 5.08, N, 7.33. Found: C, 57.12, H, 5.25, N, 7.16. ES MS found m/z 1341.5, calculated m/z 1341.6 for $[M - PF_6]^+$. HR MS found m/z 1339.5461, calculated m/z 1339.5488 for $[C_{72}H_{76}N_8O_6{}^{191}Ir]^+$.

[Ir(L^3)$_2$(bpy)]PF$_6$. This compound was prepared similarly from $[(L^3)_2Ir(\mu\text{-}Cl)_2Ir(L^3)_2]$ (0.085 g, 0.050 mmol) and 2,2′-bipyridine (0.017 g, 0.108 mmol). Yield 0.091 g (79%). ^{1}H NMR (400 MHz, $CDCl_3$) δ_H = 8.56 (2H, d, $^3J_{HH}$ = 5.5 Hz), 8.22 (2H, d, $^3J_{HH}$ = 8.1 Hz), 8.00 (2H, app. t, $^3J_{HH}$ = 7.0 Hz), 7.89 (2H, d, $^3J_{HH}$ = 8.3 Hz), 7.62 (6H, m), 7.43 (2H, app. t, $^3J_{HH}$ = 8.0 Hz), 7.36 (4H, d, $^3J_{HH}$ = 7.9 Hz), 7.17 (2H, d, $^3J_{HH}$ = 9.0 Hz), 7.09−6.94 (4H, m), 6.56 (2H, d, $^3J_{HH}$ = 8.3 Hz), 6.21 (2H, s), 2.46 (6H, s), 1.87 (6H, s) ppm. ^{13}C{^{1}H} NMR (75 MHz, $CDCl_3$) δ_C = 163.5, 155.7, 153.9, 153.0, 147.9, 142.0, 141.4, 140.8, 140.6, 140.4, 140.2, 136.7, 135.5, 131.6, 131.2, 130.3, 130.2, 130.1, 128.8, 128.1, 125.1, 124.0, 123.7, 21.8, 21.7 ppm. UV−vis (MeCN): λ_{max} (ε/dm^3 mol^{-1} cm^{-1}) 298 (39 800), 388 (19 600), 471 (4900) nm. Anal. Calcd (%) for $C_{54}H_{42}N_6IrPF_8$: C, 58.32, H, 3.81, N, 7.55. Found: C, 58.08, H, 3.95, N, 7.41. ES MS found m/z 967.3, calculated m/z 967.3 for $[M - PF_6]^+$. HR MS found m/z 965.3069, calculated m/z 965.3071 for $[C_{54}H_{42}N_6{}^{191}Ir]^+$.

■ ASSOCIATED CONTENT

Ⓢ Supporting Information

Parameters associated with the single crystal diffraction data collection, selected bond lengths and angles, ortep representation of **[Ir(L^3)$_2$(Diobpy)]$^+$**, TD-DFT data, and luminescence spectroscopy data. This material is available free of charge via the Internet at http://pubs.acs.org.

■ AUTHOR INFORMATION

Corresponding Author

*E-mail: popesj@cardiff.ac.uk. Phone: +44 (0) 29 20879316. Fax: +44 (0) 29 20874030.

Notes

The authors declare no competing financial interest.

■ ACKNOWLEDGMENTS

Cardiff University and EPSRC are thanked for funding. Dr. Robert Jenkins, Mr. Robin Hicks, and Mr. David Walker are

thanked for running low resolution mass spectra. Dr. Benson Kariuki is thanked for obtaining the raw diffraction data on $[Ir(L^3)_2(Diobpy)]PF_6$ and $[Ir(L^3)_2(bpy)]PF_6$. The staff of the EPSRC MS National Service at the University of Swansea are also gratefully acknowledged.

REFERENCES

(1) Baldo, M. A.; Thompson, M. E.; Forrest, S. R. *Nature* **2000**, *403*, 750−753.

(2) Flamigni, L.; Barbieri, A.; Sabatini, C.; Ventura, B.; Barigelletti, F. *Top. Curr. Chem.* **2007**, *281*, 143−203.

(3) (a) Beeby, A.; Bettington, S.; Samuel, I. D. W.; Wang, Z. *J. Mater. Chem.* **2003**, *13*, 80−83. (b) Hwang, F.-M.; Chen, H.-Y.; Chen, P.-S.; Liu, C.-S.; Chi, Y.; Shu, C.-F.; Wu, F.-I.; Chou, P.-T.; Peng, S.-M.; Lee, G.-H. *Inorg. Chem.* **2005**, *44*, 1344−1353. (c) Grushin, V. V.; Herron, N.; LeCloux, D. D.; Marshall, W. J.; Petrov, V. A.; Wang, Y. *Chem. Commun.* **2001**, 1494−1495. (d) Ho, C.-L.; Wong, W.-Y.; Zhou, G.-J.; Yao, B.; Xie, Z.; Wang, L. *Adv. Funct. Mater.* **2007**, *17*, 2925−2936.

(4) (a) Chen, S.; Tan, G.; Wong, W.-Y.; Kwok, H.-S. *Adv. Funct. Mater.* **2011**, *21*, 3785−3793. (b) Yu, X.-M.; Zhou, G.-J.; Lam, C.-S.; Wong, W.-Y.; Zhu, X.-L.; Sun, J.-X.; Wong, M.; Kwok, H.-S. *J. Organomet. Chem.* **2008**, *693*, 1518−1527. (c) Zhou, G.; Wang, Q.; Ho, C.-L.; Wong, W.-Y.; Ma, D.; Wang, L.; Lin, Z. *Chem.—Asian J.* **2008**, *3*, 1830−1841. (d) Wu, Z.; Xing, K.; Luo, C.; Liu, Y.; Yang, Y.; Gan, Q.; Zhu, M.; Jiang, C.; Cao, Y.; Zhu, W. *Chem. Lett.* **2006**, *35*, 538−539. (e) Jayabharathi, J.; Thanikachalam, V.; Srinivasan, N.; Perumal, M. V. *Spectrochim. Acta, Part A* **2011**, *79*, 338−347. (f) Huang, W.-S.; Lin, C.-W.; Lin, J. T.; Huang, J.-H.; Chu, C.-W.; Wu, Y.-H.; Lin, H.-C. *Org. Electron.* **2009**, *10*, 594−606. (g) Dedeian, K.; Djurovich, P. I.; Garces, F. O.; Carlson, G.; Watts, R. J. *Inorg. Chem.* **1991**, *30*, 1685−1687. (h) King, K. A.; Spellane, P. J.; Watts, R. J. *J. Am. Chem. Soc.* **1985**, *107*, 1431−1433.

(5) (a) Zhu, M.; Li, Y.; Hu, S.; Li, C.; Yang, C.; Wu, H.; Qina, J.; Caob, Y. *Chem. Commun.* **2012**, *48*, 2695−2697. (b) Duan, J. P.; Sun, P.; Cheng, C.-H. *Adv. Mater.* **2003**, *15*, 224−228. (c) Rayabarapu, D.; Paulose, B.; Duan, J. P.; Cheng, C.-H. *Adv. Mater.* **2005**, *17*, 349−353. (d) Lu, K.-Y.; Chou, H.-H.; Hsieh, C.-H.; Yang, Y-H. O.; Tsai, H.-R.; Tsai, H.-Y.; Hsu, L.-C.; Chen, C.-Y.; Chen, I. C.; Cheng, C.-H. *Adv. Mater.* **2011**, *23*, 4933−4937.

(6) (a) Tao, R.; Qiao, J.; Zhang, G.; Duan, L.; Wang, L.; Qiu, Y. *J. Phys. Chem. C* **2012**, *116*, 11658−11664. (b) Zhang, F.; Duan, L.; Qiao, J.; Dong, G.; Wang, L.; Qiu, Y. *Org. Electron.* **2012**, *13*, 1277−1288. (c) Dumur, F.; Nasr, G.; Wantz, G.; Mayer, C. R.; Dumas, E.; Guerlin, A.; Miomandre, F.; Clavier, G.; Bertin, D.; Gigmes, D. *Org. Electron.* **2011**, *12*, 1683−1694.

(7) (a) Lamansky, S.; Djurovich, P.; Murphy, D.; Abdel-Razzaq, F.; Lee, H.-E.; Adachi, C.; Burrows, P. E.; Forrest, S. R.; Thompson, M. E. *J. Am. Chem. Soc.* **2001**, *123*, 4304−4312. (b) King, K. A.; Watts, R. J. *J. Am. Chem. Soc.* **1987**, *109*, 1589−1590. (c) Dragonetti, C.; Falciola, L.; Mussini, P.; Righetto, S.; Roberto, D.; Ugo, R.; Valore, A.; De Angelis, F.; Fantacci, S.; Sgamellotti, A.; Ramon, M.; Muccini, M. *Inorg. Chem.* **2007**, *46*, 8533−8547. (d) Baranoff, E.; Yum, J.-H.; Graetzel, M.; Nazeeruddin, Md. K. *J. Organomet. Chem.* **2009**, *694*, 2661−2670. (e) Fernández-Moreira, V.; Thorp-Greenwood, F. L.; Coogan, M. P. *Chem. Commun.* **2010**, *46*, 186−202.

(8) (a) Kessler, F.; Costa, R. D.; Di Censo, D.; Scopelliti, R.; Ortí, E.; Bolink, H. J.; Meier, S.; Sarfert, W.; Grätzel, M.; Nazeeruddin, Md. K.; Baranoff, E. *Dalton Trans.* **2012**, *41*, 180−191. (b) Jayabharathi, J.; Thanikachalam, V.; Srinivasan, N.; Perumal, M. V. *Spectrochim. Acta, Part A* **2012**, *80*, 119−125. (c) Takizawa, S-y.; Perez-Bolivar, C.; Anzenbacher, P.; Murata, S. *Eur. J. Inorg. Chem.* **2012**, 3975−3979. (d) Li, X.; Lan, H.; Chen, Y.; Lv, K.; Zhang, A.; Huang, T. *Inorg. Chim. Acta* **2012**, *390*, 41−46. (e) Tamayo, A. B.; Alleyne, B. D.; Djurovich, P. I.; Lamansky, S.; Tsyba, I.; Ho, N. N.; Bau, R.; Thompson, M. E. *J. Am. Chem. Soc.* **2003**, *125*, 7377−7387. (f) Tsuboyama, A.; Iwawaki, H.; Furugori, M.; Mukaide, T.; Kamatani, J.; Igawa, S.; Moriyama, T.; Miura, S.; Takiguchi, T.; Okada, S.; Hoshino, M.; Ueno, K. *J. Am. Chem. Soc.* **2003**, *125*, 12971−12979. (g) Lo, K. K-W.; Chung, C.-K.; Lee, T. K-M.; Lui, L.-H.; Tsang, K. H-K.; Zhu, N. *Inorg. Chem.* **2003**, *42*, 6886−6897. (h) Lau, J. S-Y.; Lee, P.-K.; Tsang, K. H-K.; Ng, C. H-C.; Lam, Y.-W.; Cheng, S.-H.; Lo, K. K-W. *Inorg. Chem.* **2009**, *48*, 708−718. (i) Baranoff, E.; Fantacci, S.; De Angelis, F.; Zhang, X.; Scopelliti, R.; Graetzel, M.; Nazeeruddin, Md. K. *Inorg. Chem.* **2011**, *50*, 451−462. (j) Ma, L.; Guo, H.; Li, Q.; Guo, S.; Zhao, J. *Dalton Trans.* **2012**, *41*, 10680−10689. (k) Hallett, A. J.; White, N.; Wu, W.; Cui, X.; Horton, P. N.; Coles, S. J.; Zhao, J.; Pope, S. J. A. *Chem. Commun.* **2012**, *48*, 10838−10840. (l) Li, X.; Minaev, B.; Ågren, H.; Tian, H. *J. Phys. Chem. C* **2011**, *115*, 20724−20731. (m) Monaco, S.; Semeraro, M.; Tan, W.; Tian, H.; Ceroni, P.; Credi, A. *Chem. Commun.* **2012**, *48*, 8652−8654. (n) Li, X.; Minaev, B.; Ågren, H.; Tian, H. *Eur. J. Inorg. Chem.* **2011**, 2517−2524. (o) Li, X.; Zhang, Q.; Tu, Y.; Ågren, H.; Tian, H. *Phys. Chem. Chem. Phys.* **2010**, *12*, 13730−13736. (p) Jiang, W.; Gao, Y.; Sun, Y.; Ding, F.; Xu, Y.; Bian, Z.; Li, F.; Bian, J.; Huang, C. *Inorg. Chem.* **2010**, *49*, 3252−3260.

(9) (a) Wang, C.; Wong, K. M.-C. *Inorg. Chem.* **2011**, *50*, 5333−5335. (b) Xu, W.-J.; Liu, S.-J.; Ma, T.-C.; Zhao, Q.; Pertegás, A.; Tordera, D.; Bolink, H. J.; Ye, S.-H.; Liu, X.-M.; Sun, S.; Huang, W. *J. Mater. Chem.* **2011**, *21*, 13999−14007. (c) Park, H. R.; Ha, Y. *Mol. Cryst. Liq. Cryst.* **2011**, *538*, 67−74. (d) Schneidenbach, D.; Ammermann, S.; Debeaux, M.; Freund, A.; Zöllner, M.; Daniliuc, C.; Jones, P. G.; Kowalsky, W.; Johannes, H.-H. *Inorg. Chem.* **2010**, *49*, 397−406. (e) Bolink, H. J.; Coronado, E.; Sessolo, M. *Chem. Mater.* **2009**, *21*, 439−441. (f) Lee, H.-S.; Ahn, S. Y.; Ha, Y. *Mol. Cryst. Liq. Cryst.* **2009**, *514*, 14−24. (g) Ying, L.; Zou, J.; Yang, W.; Wu, H.; Zhang, A.; Wu, Z.; Cao, Y. *Macromol. Chem. Phys.* **2009**, *210*, 457−466. (h) Ahn, S. Y.; Lee, H. S.; Seo, J.-H.; Kim, Y. K.; Ha, Y. *Thin Solid Films* **2009**, *517*, 4111−4114. (i) Ge, G.; Zhang, G.; Guo, H.; Chuai, Y.; Zou, D. *Inorg. Chim. Acta* **2009**, *362*, 2231−2236. (j) Lee, H. S.; Ahn, S. Y.; Seo, J.-H.; Kim, Y.-K.; Ha, Y. *J. Korean Phys. Soc.* **2009**, *55*, 1977−1981. (k) Ha, Y.; Seo, J.-H.; Kim, Y. K. *Synth. Met.* **2008**, *158*, 548−552. (l) Mao, C.-H.; Hong, J.-L.; Yeh, A.-C. *J. Polym. Sci., Part B: Polym. Phys.* **2008**, *46*, 631−639. (m) Tani, K.; Fujii, H.; Mao, L.; Sakurai, H.; Hirao, T. *Bull. Chem. Soc. Jpn.* **2007**, *80*, 783−788. (n) Chen, H.-Y.; Yang, C.-H.; Chi, Y.; Cheng, Y.-M.; Yeh, Y.-S.; Chou, P.-T.; Hsieh, H.-Y.; Liu, C.-S.; Peng, S.-M.; Lee, G.-H. *Can. J. Chem.* **2006**, *84*, 309−318. (o) Gao, J.; You, H.; Fang, J.; Ma, D.; Wang, L.; Jing, X.; Wang, F. *Synth. Met.* **2005**, *155*, 168−171. (p) Zhang, G.-L.; Guo, H.-Q.; Chuai, Y.-T.; Zou, D.-C. *Acta Chim. Sin.* **2005**, *63*, 143−147. (q) Zhang., G. L.; Liu, Z. H.; Guo, H. Q. *Chin. Chem. Lett.* **2004**, *15*, 1349−1352. (r) Ahn, S.-Y.; Seo, J.-H.; Kim, Y.-K.; Ha, Y. *J. Nanosci. Nanotechnol.* **2009**, *9*, 7039−7043. (s) Wiegmann, B.; Jones, P. G.; Wagenblast, G.; Lennartz, C.; Muenster, I.; Metz, S.; Kowalsky, W.; Johannes, H.-H. *Organometallics* **2012**, *31*, 5223−5226. (t) Jones, P. G.; Ammermann, S.; Daniliuc, C.; du Mont, W.-W.; Kowalsky, W.; Johannes, H.-H. *Acta Crystallogr., Sect. E* **2006**, *62*, m2202−m2204. (u) Chang, Y.-L.; Wang, Z. B.; Helander, M. G.; Qiu, J.; Puzzo, D. P.; Lu, Z. H. *Org. Electron.* **2012**, *13*, 925−931.

(10) Routledge, J. D.; Hallett, A. J.; Platts, J. A.; Horton, P. N.; Pope, S. J. A. *Eur. J. Inorg. Chem.* **2012**, 4065−4075.

(11) Hallett, A. J.; Kariuki, B. M.; Pope, S. J. A. *Dalton Trans.* **2011**, *40*, 9474−9481.

(12) (a) Hallett, A. J.; Jones, J. E. *Dalton Trans.* **2011**, *40*, 3871−3876. (b) Vickers, M. S.; Martindale, K. S.; Beer, P. D. *J. Mater. Chem.* **2005**, *15*, 2784−2790. (c) Hamada, T.; Tanaka, S.-I.; Koga, H.; Sakai, Y.; Sakaki, S. *Dalton Trans.* **2003**, 692−698.

(13) (a) Lindsley, C. W.; Zhao, Z.; Leister, W. H.; Robinson, R. G.; Barnett, S. F.; Defeo-Jones, D.; Jones, R. E.; Hartman, G. D.; Huff, J. R.; Huber, H. E.; Duggan, M. E. *Bioorg. Med. Chem. Lett.* **2005**, *15*, 761−764. (b) Prakash, G. *Future Med. Chem.* **2009**, *1*, 909−920.

(14) Loriga, M.; Piras, S.; Sanna, P.; Paglietti, G. *Farmaco* **1997**, *52*, 157−166.

(15) (a) Seitz, L. E.; Suling, W. J.; Reynolds, R. C. *J. Med. Chem.* **2002**, *45*, 5604−5606. (b) Murthy, Y. L. N.; Mani, P.; Govindh, B.; Diwakar, B. S.; Karthikeyan, N.; Rao, T. R.; Rao, K. V. R. *Res. J. Pharm., Biol. Chem. Sci.* **2011**, *2*, 553−560.

(16) (a) He, W.; Myers, M. R.; Hanney, B.; Spada, A. P.; Bilder, G.; Galzcinski, H.; Amin, D.; Needle, S.; Page, K.; Jayyosi, Z.; Perrone, M.

H. *Bioorg. Med. Chem. Lett.* **2003**, *13*, 3097−3100. (b) Gazit, A.; App, H.; McMahon, G.; Chen, J.; Levitzki, A.; Bohmer, F. D. *J. Med. Chem.* **1996**, *39*, 2170−2177.
(17) (a) Chandrasekaran, Y.; Dutta, G. K.; Kanth, R. B.; Patil, S. *Dyes Pigm.* **2009**, *83*, 162−167. (b) Son, H.-J.; Han, W.-S.; Yoo, D.-H.; Min, K.-T.; Kwon, S.-N.; Ko, J.; Kang, S. O. *J. Org. Chem.* **2009**, *74*, 3175−3178. (c) Brock, E. D.; Lewis, D. M.; Yousaf, T. I.; Harper, H. H. (The Procter and Gamble Company). WO 9951688, 1999.
(18) (a) Kulkarni, A. P.; Zhu, Y.; Jenekhe, S. A. *Macromolecules* **2005**, *38*, 1553−1563. (b) Thomas, K. R. J.; Lin, J. T.; Tao, Y.-T.; Chuen, C.-H. *Chem. Mater.* **2002**, *14*, 2796−2802. (c) Wang, H.; Chen, G.; Liu, Y.; Hu, L.; Xu, X.; Ji, S. *Dyes Pigm.* **2009**, *83*, 269−275. (d) Sun, M.; Jiang, X.; Liu, W.; Zhu, T.; Huang, F.; Cao, Y. *Synth. Met.* **2012**, *162*, 1406−1410.
(19) (a) Steel, P. J.; Caygill, G. B. *J. Organomet. Chem.* **1990**, *395*, 359−373. (b) Karastatiris, P.; Mikroyannidis, J. A.; Spiliopoulos, I. K. *Macromolecules* **2004**, *37*, 7867−7878. (c) More, S. V.; Sastry, M. N. V.; Wang, C.-C.; Yao, C.-F. *Tetrahedron Lett.* **2005**, *46*, 6345−6348. (d) Kaupp, G.; Naimi-Jamal, M. R. *Eur. J. Org. Chem.* **2002**, 1368−1373.
(20) Nonoyama, M. *Bull. Chem. Soc. Jpn.* **1974**, *47*, 767−768.
(21) (a) Hallett, A. J.; Ward, B. D.; Kariuki, B. M.; Pope, S. J. A. *J. Organomet. Chem.* **2010**, *695*, 2401−2409. (b) Lamansky, S.; Djurovich, P.; Murphy, D.; Abdel-Razzaq, F.; Kwong, R.; Tsyba, I.; Bortz, M.; Mui, B.; Bau, R.; Thompson, M. E. *Inorg. Chem.* **2001**, *40*, 1704−1711. (c) Garces, F. O.; King, K. A.; Watts, R. J. *Inorg. Chem.* **1998**, *27*, 3464−3471.
(22) (a) Neve, F.; Crispini, A.; Campagna, S.; Serroni, S. *Inorg. Chem.* **1999**, *38*, 2250−2258. (b) Ladouceur, S.; Fortin, D.; Zysman-Colman, E. *Inorg. Chem.* **2010**, *49*, 5625−5641.
(23) (a) Mishra, A.; Nayak, P. K.; Ray, D.; Patankar, M. P.; Narasimhan, K. L.; Periasamy, N. *Tetrahedron Lett.* **2006**, *47*, 4715−4719. (b) Andrade, B. W. D.; Datta, S.; Forrest, S. R.; Djurovich, P.; Polikarpov, E.; Thompson, M. E. *Org. Electron.* **2005**, *6*, 11−20.
(24) Ruggi, A.; van Leeuwen, F. W. B.; Velders, A. H. *Coord. Chem. Rev.* **2011**, *255*, 2542−2554 and references therein.
(25) (a) Frank, M.; Nieger, M.; Vogtle, F.; Belser, P.; von Zelewsky, A.; Cola, L. D.; Balzani, V.; Barigelletti, F.; Flamigni, L. *Inorg. Chim. Acta* **1996**, *242*, 281−291. (b) Juris, A.; Balzani, V.; Barigelletti, F.; Campagna, S.; Belser, P.; von Zelewsky, A. *Coord. Chem. Rev.* **1988**, *84*, 85−277.
(26) Connelly, N. G.; Geiger, W. E. *Chem. Rev.* **1996**, *96*, 877−910.
(27) *SHELXL-PC Package*; Bruker Analytical X-ray Systems: Madison, WI, 1988.
(28) Frisch, M. J.; Trucks, G. W.; Schlegel, H. B.; Scuseria, G. E.; Robb, M. A.; Cheeseman, J. R.; Montgomery, J. A., Jr.; Vreven, T.; Kudin, K. N.; Burant, J. C.; Millam, J. M.; Iyengar, S. S.; Tomasi, J.; Barone, V.; Mennucci, B.; Cossi, M.; Scalmani, G.; Rega, N.; Petersson, G. A.; Nakatsuji, H.; Hada, M.; Ehara, M.; Toyota, K.; Fukuda, R.; Hasegawa, J.; Ishida, M.; Nakajima, T.; Honda, Y.; Kitao, O.; Nakai, H.; Klene, M.; Li, X.; Knox, J. E.; Hratchian, H. P.; Cross, J. B.; Bakken, V.; Adamo, C.; Jaramillo, J.; Gomperts, R.; Stratmann, R. E.; Yazyev, O.; Austin, A. J.; Cammi, R.; Pomelli, C.; Ochterski, J. W.; Ayala, P. Y.; Morokuma, K.; Voth, G. A.; Salvador, P.; Dannenberg, J. J.; Zakrzewski, V. G.; Dapprich, S.; Daniels, A. D.; Strain, M. C.; Farkas, O.; Malick, D. K.; Rabuck, A. D.; Raghavachari, K.; Foresman, J. B.; Ortiz, J. V.; Cui, Q.; Baboul, A. G.; Clifford, S.; Cioslowski, J.; Stefanov, B. B.; Liu, G.; Liashenko, A.; Piskorz, P.; Komaromi, I.; Martin, R. L.; Fox, D. J.; Keith, T.; Al-Laham, M. A.; Peng, C. Y.; Nanayakkara, A.; Challacombe, M.; Gill, P. M. W.; Johnson, B.; Chen, W.; Wong, M. W.; Gonzalez, C.; Pople, J. A. *Gaussian 03, Revision E.01*; Gaussian, Inc.: Wallingford CT, 2004.
(29) (a) Hay, P. J.; Wadt, W. R. *J. Chem. Phys.* **1985**, *82*, 270−283. (b) Hay, P. J.; Wadt, W. R. *J. Chem. Phys.* **1985**, *82*, 299−310.
(30) (a) Francl, M. M.; Pietro, W. J.; Hehre, W. J.; Binkley, J. S.; DeFrees, D. J.; Pople, J. A.; Gordon, M. S. *J. Chem. Phys.* **1982**, *77*, 3654−3665. (b) Hariharan, P. C.; Pople, J. A. *Theor. Chem. Acc.* **1973**, *28*, 213−222.
(31) Ditchfield, R.; Hehre, W. J.; Pople, J. A. *J. Chem. Phys.* **1971**, *54*, 724−728.
(32) Tomasi, J.; Mennucci, B.; Cammi, R. *Chem. Rev.* **2005**, *105*, 2999−3094 and references therein..
(33) Brown, D. J. Quinoxalines: Supplement II. In *The Chemistry of Heterocyclic Compounds*; Taylor, E. C., Wipf, P., Eds.; John Wiley & Sons: Hoboken, NJ, 2004.